NeuroImage: Clinical 28 (2020) 102431

Contents lists available at ScienceDirect

NeuroImage: Clinical

journal homepage: www.elsevier.com/locate/ynicl

Altered dynamic effective connectivity of the default mode network in newly diagnosed drug-naïve juvenile myoclonic epilepsy

Zhe Zhang[a,1], Guangyao Liu[b,1], Weihao Zheng[a], Jie Shi[c], Hong Liu[b], Yu Sun[a,d,*]

[a] Key Laboratory for Biomedical Engineering of Ministry of Education, Department of Biomedical Engineering, Zhejiang University, Zhejiang, China
[b] Department of Magnetic Resonance, Lanzhou University Second Hospital, Lanzhou, China
[c] School of Information Science and Engineering, Lanzhou University, Lanzhou, China
[d] Department of Radiology, Children's Hospital, Zhejiang University School of Medicine, National Clinical Research Center for Child Health, Zhejiang, China

ARTICLE INFO

Keywords:
Juvenile myoclonic epilepsy
Newly diagnosed drug-naïve
Default mode network
Dynamic effective connectivity

ABSTRACT

Juvenile myoclonic epilepsy (JME) has been repeatedly revealed to be associated with brain dysconnectivity in the default mode network (DMN). However, the implicit assumption of stationary and nondirectional functional connectivity (FC) in most previous resting-state fMRI studies raises an open question of JME-related aberrations in dynamic causal properties of FC. Here, we introduces an empirical method incorporating sliding-window approach and a multivariate Granger causality analysis to investigate, for the first time, the reorganization of dynamic effective connectivity (DEC) in DMN for patients with JME. DEC was obtained from resting-state fMRI of 34 patients with newly diagnosed and drug-naïve JME and 34 matched controls. Through clustering analysis, we found two distinct states that characterize the DEC patterns (i.e., a less frequent, strongly connected state (State 1) and a more frequent, weakly connected state (State 2)). Patients showed altered ECs within DMN subnetworks in the State 2, whereas abnormal ECs between DMN subnetworks were found in the State 1. Furthermore, we observed that the causal influence flows of the medial prefrontal cortex and angular gyrus were altered in a manner of state specificity, and associated with disease severity of patients. Overall, our findings extend the dysconnectivity hypothesis in JME from static to dynamic causal FC and demonstrate that aberrant DEC may underlie abnormal brain function in JME at early phase of illness.

1. Introduction

Juvenile myoclonic epilepsy (JME), characterized by myoclonic jerks of upper limbs after awakening, is the most common idiopathic generalized epilepsy (IGE) syndrome in adults, accounting for up to 10% of all epilepsy cases (Inanaga et al., 1985; Panayiotopoulos et al., 1994; Scheffer et al., 2017). Although response to appropriate anti-epileptic drugs (AEDs) is good, more patients seem to relapse after stopping AEDs than in any other epilepsy syndrome (Koepp et al., 2014). Patients with JME typically show various cognitive impairments, such as deficits in working memory, attention, and executive functions (Carvalho et al., 2016; Pascalicchio et al., 2007; Wandschneider et al., 2012), and these cognitive impairments severely affect patients' quality of life and to some extent increase social and economic burden. Because of these apparent cognitive comorbidities, continuous efforts have been made to understand the fundamental mechanisms underlying the neuropsychology of JME (Caciagli et al., 2019; Jiang et al., 2018; Wandschneider et al., 2019).

With advances in functional magnetic resonance imaging (fMRI) techniques, researchers have made significant progress in understanding the pathogenesis of JME (Baykan and Wolf, 2017; Wolf et al., 2015). There has been ample evidence of disrupted brain networks, including thalamo-cortical, fronto-insula, default modal, basal ganglia, sensorimotor networks, etc., in JME patients (Dong et al., 2016; Gleichgerrcht et al., 2015; Lee and Park, 2019; O'Muircheartaigh et al., 2012; Paulus et al., 2015; Wang et al., 2019; Zhong et al., 2018). However, studying the dysfunctions of brain networks in patients who have been treated with AEDs makes it difficult to differentiate brain changes caused by the disease itself from a potential prominent changes caused by AEDs. Thus, it is extremely essential to identify the changes of brain networks at early phase of the disease without the confounding effects of pharmacological treatment.

* Corresponding author at: Key Laboratory for Biomedical Engineering of Ministry of Education, Department of Biomedical Engineering, Zhejiang University, Zhejiang 310000, China.
E-mail address: yusun@zju.edu.cn (Y. Sun).
[1] These authors have contributed equally to this work.

https://doi.org/10.1016/j.nicl.2020.102431
Received 18 June 2020; Received in revised form 8 August 2020; Accepted 8 September 2020
Available online 11 September 2020
2213-1582/ © 2020 Published by Elsevier Inc. This is an open access article under the CC BY-NC-ND license (http://creativecommons.org/licenses/BY-NC-ND/4.0/).

The default mode network (DMN) that is activated in a task-free state and suppressed during passive tasks, plays a pivotal role in many cognitive processes, such as remembering, envisioning the future and making social inferences (Akansha et al., 2016; Buckner and DiNicola, 2019). The main cortical regions within the DMN include the medial prefrontal cortex (MPFC), posterior cingulate gyrus (PCC), precuneus (PCU), inferior parietal cortex, and hippocampus (Mason et al., 2007). Functional disruption of the DMN have been recently revealed in patients with JME. For example, patients with JME showed decreased functional interactions between the PCC and MPFC (McGill et al., 2012); the coupling of spontaneous fluctuation and functional connectivity (FC) in posterior regions of the DMN was altered in patients and associated with clinical symptoms during seizures (Jia et al., 2018); aberrant FC in hippocampus was also involved in the cognitive dysregulation of JME (Zhong et al., 2018). Taken together, these findings suggested that the DMN is prominently affected in patients with JME (Parsons et al., 2020), and a specific investigation targeting DMN may lead new insights to revealing the pathogenesis of JME at the early phase of this disorder. It is noteworthy mentioning that the above-mentioned studies have measured FC by estimating the full time courses over the entire scan, and thus blurred the dynamic properties of brain activity over time.

The functional interaction in the brain is known to be highly dynamic rather than static (Calhoun et al., 2014; Lurie et al., 2020). The dynamic FC therefore is considered to be a more efficient way for uncovering specific functional integration properties in healthy and disease (Allen et al., 2014; Damaraju et al., 2014; Fu et al., 2019; Kim et al., 2017; Malhi et al., 2019; Tu et al., 2019). The dynamic FC analysis have been utilized to explore time-varying abnormalities of resting-state networks (RSNs) in different subtypes of IGE as well as JME. For example, children with absence seizure (AS) showed altered dynamic connectivity maps in the thalamic network and the DMN across three different seizure intervals (Liao et al., 2014); state-specific connectivity disruptions that mainly related to DMN were observed in patients with generalized tonic-clonic seizures (GTCS) (Liu et al., 2017). For patients with JME, hyper dynamic characteristics in temporally fluctuating functional networks have been found (Wang et al., 2019). Our previous study also demonstrated altered FC dynamics within and between RSNs, which were associated with the disease severity of JME patients (Zhang et al., 2018). These studies suggested aberrant dynamic connectivity patterns of RSNs, particularly the DMN, are remarkable characteristics in patients with IGE. However, previous dynamic studies only characterized FC based on the temporal correlation between brain signals, ignoring the causal influences among brain regions (e.g., the influence of one brain regions on another (Friston, 2011)) that may provide more reasonable evidence for diagnosis, prognosis, and assessment of treatment responses of neurological and psychiatric disorders (Dobryakova et al., 2017; Hamilton et al., 2011; Mastrovito et al., 2018; Park et al., 2018a; Sladky et al., 2015). To the best of our knowledge, no study has explored dynamic effective connectivity (DEC) in patients with JME, and the time-varying aspect of the causal influences among DMN regions for this disorder remains unclear.

The primary aim of this study is to investigate the differences in DEC within the DMN between healthy controls and patients with newly diagnosed and drug-naïve JME. To achieve this goal, we identified the default mode (DM) components by using a group independent component analysis (gICA), and then characterized DEC among the DM components by combining a sliding window approach with multivariate Granger causality analysis (mGCA). We further evaluated causal influence flows of DM components as well as temporal properties of dynamic states after clustering all DEC matrices into two EC states. Our DEC approach offers a practical way of examining the temporal patterns of the DMN connectivity in JME. Based upon the previous literature describing dysconnectivity of DMN and abnormalities of dynamic FC in JME, we hypothesized that patients with JME would exhibit atypical dynamic causal influence and temporal properties in the DMN vs. healthy controls, and these abnormal DEC patterns would be linked to clinical severity of JME.

2. Materials and methods

2.1. Participants

The study sample consisted of 38 patients with newly diagnosed JME recruited at the Epilepsy Center of Lanzhou University Second Hospital between August 2016 and June 2018 and 37 matched healthy controls recruited from the local community through advertisements. The patients were diagnosed as JME based on the epilepsy classification criteria of the International League Against Epilepsy (ILAE) guidelines (Jr, 2001). Routine MRI scans were normal, and routine scalp EEG showed 3–6 Hz generalized spike-wave or polyspike-wave discharges (GSWDs). Patients were excluded if they had any of the following characteristics: 1) a history of antiepileptic medication-intake, 2) had other neurological or psychiatric illness, 3) had other developmental disabilities, such as autism and intellectual impairment, and 4) had acute physical illness that would affect the scanning. To assess seizure severity, each patient was requested to perform the National Hospital Seizure Severity Scale (NHS3) prior to the MRI scans. The NHS3 measures seizure severity in a manner compatible with the subjective impression of people with epilepsy, focusing solely on the objective clinical events of a seizure (O' Donoghue et al., 1996). It contains six seizure-related factors and generates a total score from 1 to 23. Healthy controls were additionally screened for history of febrile convulsions, seizures, or family history for epilepsy. This study was approved by the Ethics Committee of Lanzhou University Second Hospital. Written informed consent was obtained from each participant or one of his/her legal guardians after the explanation of the experimental protocol prior to imaging.

2.2. Data acquisition

MRI data were acquired on a Siemens Verio 3.0 T scanner (Siemens, Erlangen, Germany) with 16 head-coil at the Department of Magnetic Resonance of Lanzhou University Second Hospital. Participants were instructed to keep still and remain as motionless as possible before the scanning. Participants were additionally required to stay awake with their eyes closed and not to think systematically during the scan. In order to further minimize the head motion, form pads provided by the scanner manufacturer were used to fix the head. Resting-state functional images were acquired for each participant using an echo-planar imaging sequence with the following settings: repetition time [RT] = 2000 ms; echo time [TE] = 30 ms; flip angle = 90°; slice thickness = 4 mm; in-plane matrix resolution = 64 × 64; field of view [FOV] = 240 × 240 mm^2; slices = 33; number of total volumes = 200. For anatomical localization and normalization, high-resolution structural 3D T1-weighted images were obtained using a magnetization-prepared rapid gradient-echo sequence (TR = 1900 ms; TE = 2.99 ms; flip angle = 90°; slice thickness = 0.9 mm; acquisition matrix = 256 × 256; FOV = 230 × 230 mm^2; in-plane resolution = 0.9 × 0.9 mm^2; slices = 192).

2.3. Data preprocessing

Resting-state functional images were preprocessed using DPARSF software (http://www.restfmri.net) based on SPM12 (http://www.fil.ion.ucl.ac.uk/spm). The main procedures included discard of the first 10 functional images, realignment, time-slicing and head motion correction, spatial normalization into the Montreal Neurological Institute (MNI) space, and spatial smoothing using a Gaussian kernel of 6 mm full width at half maximum. To minimize the effects of head motion on the estimation of dynamic EC, participants were excluded if they had: (1) head movement over than 2 mm translation or 2° rotation and (2)

Table 1
Demographic and clinical characteristics of all participants.

	JME (n = 34)	HC (n = 34)	*P* value
Age (years)	17.38 ± 4.73	19.15 ± 3.46	0.21[a]
Gender (males/females)	17/17	11/23	0.14[b]
Handedness (right/left)	34/0	34/0	–
Seizure semiology	MS (34), GTCS (24)	–	–
Age at seizure onset (year)	15.29 ± 3.44	–	–
Duration of epilepsy (months)	23.76 ± 18.99	–	–
NHS3 total score	8.65 ± 3.92	–	–
Generalized convulsions	2.82 ± 1.85	–	–
Falls	1.50 ± 1.39	–	–
Incontinence	0.32 ± 0.81	–	–
Loss of consciousness	1.41 ± 0.82	–	–
Duration of recovery time	0.97 ± 0.67	–	–
Automatisms	0.68 ± 1.06	–	–
Mean FD	0.12 ± 0.05	0.11 ± 0.04	0.45[a]

Note: [a] two sample *t*-test, [b] chi-square *t* test; Values are mean ± SD.
Abbreviations: MS, myoclonic seizure; GTCS, generalized tonic-clonic seizure; NHS3, national hospital seizure severity scale; FD, frame-wise displacement; JME, juvenile myoclonic epilepsy; HC, healthy control.

mean frame-wise displacement (FD) over than 0.3 mm. Seven participants (4 patients and 3 controls) failed to pass these criteria were excluded due to excessive head motion during MRI scanning. The detailed demographic and clinical characteristics of the included participants are shown in Table 1 and Supplementary Table S1.

2.4. Overview of dynamic effective connectivity analysis

A schematic diagram of the analysis framework to investigate atypical dynamic EC of the DMN in JME was presented in Fig. 1. Specifically, there were four major analysis steps in this framework. First, a group independent component analysis (ICA) was performed to decompose the preprocessed functional data into multiple independent components (ICs) and the DM components were identified according to their spatial activation maps. Second, to measure DEC among DM components, the time courses of DM components were divided into a set of windows by using a sliding window approach, and then the causal influence matrix in each window was constructed by using a multivariate Granger causality analysis (mGCA). Third, a k-means clustering method was implemented to cluster all DEC matrices into discrete EC states, which represented transient causal influences patterns during data acquisition time. Finally, state-specific causal influence flows among DM components and temporal properties of dynamic states were evaluated for each participant and their group differences between patients and controls were further compared. The detailed methods used for DEC analysis were provided in the following subsections.

2.5. Group independent component analysis

After data preprocessing, resting-sate data of all participants were decomposed into multiple ICs using spatial GICA with GIFT software (http://icatb.sourceforge.net/). The principal component analysis was first applied to reduce subject-specific data into 120 principal components, and then all participant-reduced data across time was concatenated and decomposed into 100 ICs using the infomax algorithm (Bell and Sejnowski, 1995). The infomax ICA algorithm was repeated 20 times in ICASSO to ensure the reliability and stability. After estimating the group spatial maps, a back reconstruction approach was used to obtain subject-specific spatial maps and corresponding time courses. We then applied a combination of spatial template-matching and visual inspection to identify DM components. Templates were derived from the ICA analyses as described in previous studies (Allen et al., 2014; Liu et al., 2017). Components were further evaluated according to the following criteria: 1) peak activation coordinates were located primarily in gray matter; 2) low spatial overlap with known

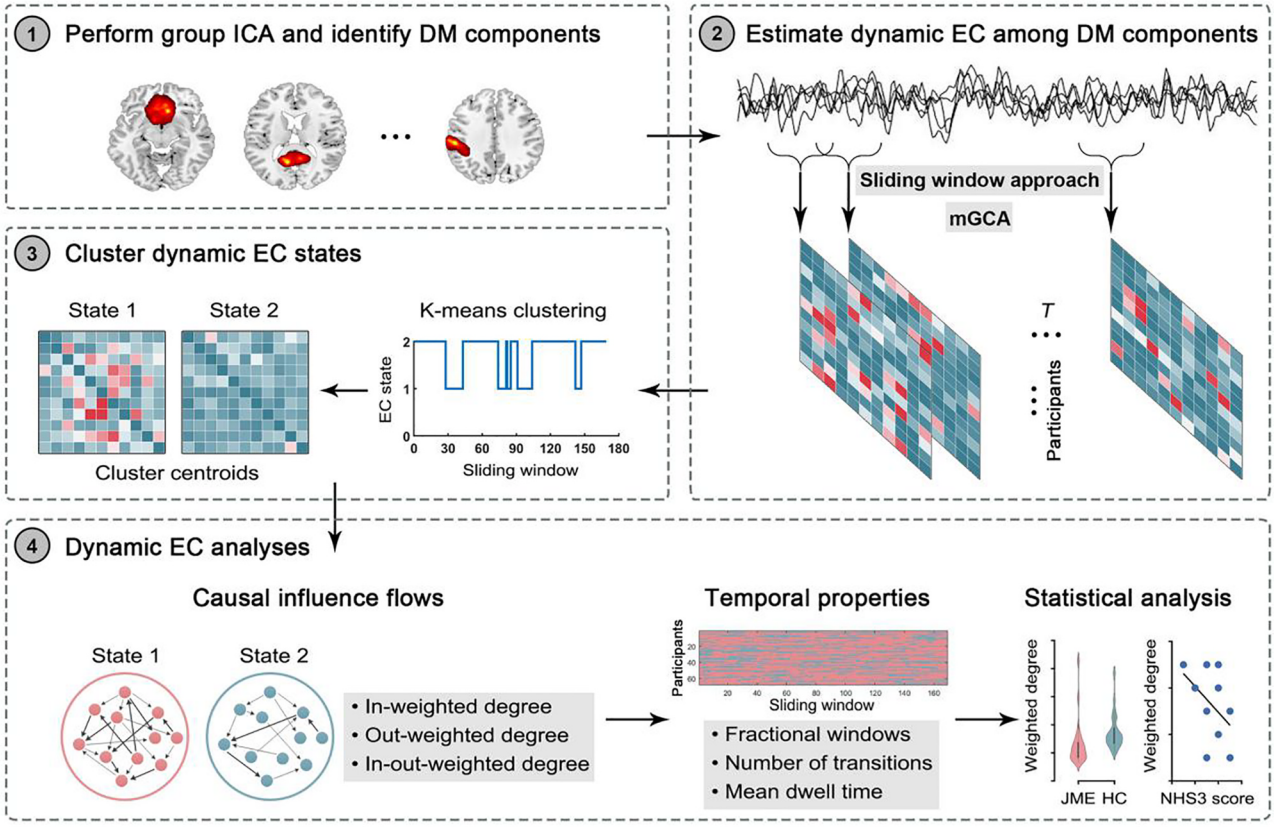

Fig. 1. Analysis flowchart to study dynamic effective connectivity of the default mode network in patients with juvenile myoclonic epilepsy.

vascular, ventricular, motion, and susceptibility artifacts; and 3) time courses were dominated by low-frequency fluctuations (Allen et al., 2011). Moreover, to remove remaining noise sources, a post-processing was performed on the time courses of selected DM components, including detrended linear, quadratic and cubic trends, regressed out six realignment parameters and their temporal derivatives, despiked detected outliers using 3DDESPIKE algorithm, and low-pass filtered with a cutoff frequency of 0.15 Hz.

2.6. Dynamic effective connectivity estimation

2.6.1. Multivariate Granger causality analysis

As a popular method for predicting causal influence of one system exerts over another, the Granger causality analysis (GCA) has been widely used to explore EC between brain regions in resting-state fMRI data (David et al., 2008; Deshpande and Hu, 2012). Different from other measures of EC, GCA quantified the causal influence among multiple brain regions in a data-driven way without requiring any predefined model (Deshpande and Hu, 2012). The idea of GCA can be simply depicted as, for two time signals $s_1(t)$ and $s_2(t)$, if knowing the past information of $s_1(t)$ could help to predict the future of $s_2(t)$, $s_1(t)$ has a causal influence on $s_2(t)$. In this study, the causal influences among the time courses of DM components were evaluated using the mGCA method (Liao et al., 2011). For each participant, the time courses set was defined as $S(t) = (s_1(t), s_2(t), \ldots, s_n(t))$, where n denotes the number of DM components. The influence from all other seed components to target component k was evaluated by the multivariate auto-regressive model as follow:

$$s_k(t) = \sum_{m=1}^{p} C_k(m)S(t-m) + R_k(t)$$

where p, C_k, S and R denote the auto-regressive model order, model coefficient matrix, time courses matrix of different components and residual error matrix, respectively. The model order p was determined using Akaike's information criterion and the model coefficient matrix C_k was calculated using a standard least squares optimization. To assess the statistical significance of Granger causality results, random-effect Granger causality maps were further calculated for each participant. The statistical thresholds for these maps were corrected with false discovery rate ($P < 0.05$).

2.6.2. Sliding window approach

The DEC among DM components was estimated using the sliding window approach, which is the most common way to investigate dynamics of brain connectivity in previous studies. A tapered window was created by convolving a rectangle window of 22 TRs (44 s) size with a Gaussian ($\sigma = 3$), and then slid it along time in steps of 1 TR, resulting in total 169 windows for each participant across the entire scan (190 TRs). Particularly, the window size of 22 TRs was selected because it has been demonstrated to provide a good cutoff between the ability of dynamics detection and the quality of correlation matrix estimation (Allen et al., 2014). Using the time courses of all DM components within each window, 169 EC matrices with $n \times n$ size were obtained for each participant, representing the dynamic changes of EC within DMN during resting-state data acquisition time. Since previous studies suggested that dynamic connectivity patterns could be captured stably in the range of 30 to 60 s, DEC was also estimated in other window sizes, such as 15, 18, 20, 25, 28, and 30 TRs to validate our main results.

2.6.3. Clustering analysis

To identify the reoccurring DEC states (depicting transient EC patterns over time), a k-means clustering method was performed on the windowed EC matrices for all participants. These matrices were categorized into a set of distinct clusters (corresponding different states) based on the similarity between matrices and cluster centroids. Here, the similarity was measured using the L1 distance (Manhattan distance) function, which is a practical method for high dimensional data (Aggarwal et al., 2001). The k-means clustering algorithm was repeated 100 times to reduce the random selection bias of initialized centroid position. The optimal number of clusters was estimated using the silhouette statistic (defined as the ratio of similarity between windows in the same cluster to similarity with windows in a different cluster) and the gap statistic (defined as the standardized pooled within-cluster sum of squares in within-cluster dispersion that is expected under a reference null distribution). In addition, the state was considered as a reliable state when it covered at least 10 windows in this study.

2.7. Causal influence flows analysis and temporal properties analysis

We performed a causal influence flows analysis to investigate state-specific directed interactions among DM components and compared it between patients and controls. Two weighted degree measures including in-weighted degree and out-weighted degree, the most common used measures of causal influence flows (Stevens et al., 2009), were calculated in each state. Here, we defined in-weighted degree of a component (or node) as the sum of influence strength from any other component to it, while defined out-weighted degree of a component as the sum of influence strength from it to any other component. In general, the component with high in-weighted degree (out-weighted degree) was considered to be a hub receptor (hub generator) of the network and often played an important role in functional integration. To assess net influence for each component, we further calculated the in-out-weighted degree on DEC matrices, which is defined as the subtraction of in-weighted degree and out-weighted degree.

In line with previous studies (Kim et al., 2017; Yao et al., 2019), we computed three different variables including fractional windows, number of transitions, and mean dwell time to evaluate the temporal properties of DEC states for each participant. Specifically, the fractional windows was defined as the proportion of windows belonging to each state, the number of transitions was defined as the transition times between states and represented the stability over time, and the mean dwell time was defined as the average number of consecutive windows belonging to each state and represented the staying time in a certain state.

2.8. Statistical analysis

The group differences in DEC parameters, including state-specific EC patterns, causal influence flows among DM components, and temporal properties of DEC states, were explored using two-sample t-test. Furthermore, Spearman's correlation analyses were applied to investigate the relationships between altered DEC parameters and clinical features in JME patients, with age, gender, and mean FD regressed out. Statistical analyses were performed using SPSS 21.0 and results were corrected for multiple comparisons using false discovery rate (FDR; $P < 0.05$).

3. Results

3.1. Default mode components

Eleven ICs were identified as DM components, located in multiple brain regions including the medial frontal gyrus (MFG; IC19, IC51, and IC87), hippocampus (Hip; IC41), anterior cingulate cortex (ACC; IC42), precuneus (PCU; IC48 and IC50), angular gyrus (Ang; IC66 and IC81), posterior cingulate cortex (PCC; IC73), and inferior parietal lobule (IPL; IC91). According to their spatial locations, these components can be further divided into two subnetworks such as anterior DMN (IC19, IC42, IC51, and IC87) and posterior DMN (IC41, IC48, IC50, IC66, IC81, IC 73, and IC91). The spatial maps of the DM components are shown in Fig. 2A. We also computed the group averaged static causal influences

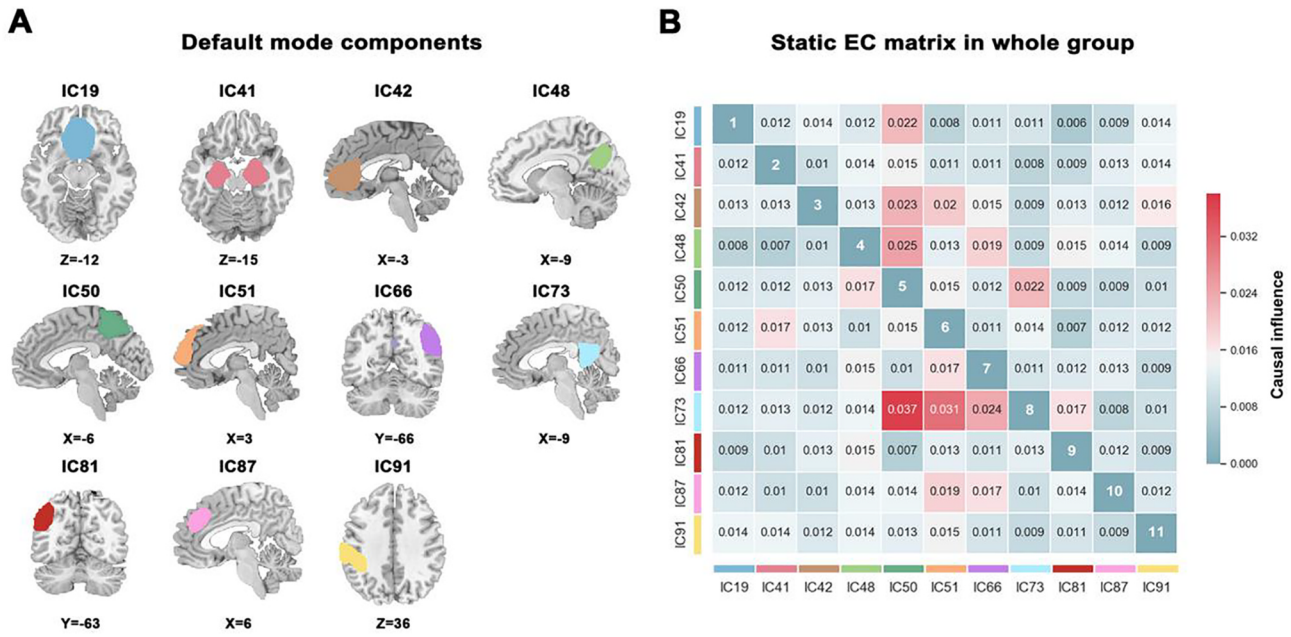

Fig. 2. Default mode components identified by a group independent component analysis. (A) Eleven independent components (ICs) were defined as default mode components according to their spatial activation maps. (B) Group averaged static effective connectivity (EC) between default mode component pairs was computed using an entire scan. The color-coded legend located on the left and at the bottom side of the matrix in (B) matches the overlaid colors of the spatial maps in (A).

among DM components over the entire scan and the corresponding EC matrix is shown in Fig. 2B. The detailed information of these DM components is provided in Supplementary Table S2.

3.2. Effective connectivity patterns in dynamic states

Two structured EC states across all participants were identified using the k-means clustering method. As shown in Fig. 3, the DEC patterns (cluster centroids) among DM components are very different between the two states. Specifically, in State 1, the DEC pattern showed stronger inter-influence but lower percentages of total occurrences (31.03%), whereas in State 2, the DEC pattern showed weaker inter-influence but more frequently total occurrences (68.97%). We also estimated and clustered DEC matrices with other sliding window sizes, and found that the DEC patterns were consistent across different sliding window sizes (see details in Supplementary Figure S1).

Fig. 4 shows state- and group-specific DEC patterns. Compared with controls, patients with JME exhibited increased EC from IC50 to IC42 and decreased EC from IC81 to IC51 in State 1; and showed increased EC from IC51 to IC42 and decreased EC from IC81 to IC66 as well as from IC66 to IC48 in State 2 (Fig. 4B, $P < 0.05$ with FDR corrected). We also observed that these changed ECs in State 1 were located between DMN subnetworks, while in State 2 were located within DMN subnetworks.

3.3. Group differences of causal influence flows and temporal properties

The group differences of causal influence flows among DM components in each state are shown in Fig. 5. In State 1, compared with controls, patients exhibited significantly decreased in-weighted degree from other DM components to IC51, decreased out-weighted degree from IC81 to other DM components, and decreased in-out-weighted degree of IC51 ($P < 0.05$, FDR corrected). In State 2, patients exhibited significantly increased out-weighted degree from IC51 to other

Fig. 3. Clustering analysis results for each state across the entire group. (A) Centroid matrices for two states. The total number of occurrences and the percentage of total occurrences are listed above each centroid matrix. (B) The difference of the mean value of absolute EC between two states. Horizontal solid and dashed lines indicate state means and interquartile range, respectively. **** represents $P < 0.0001$.

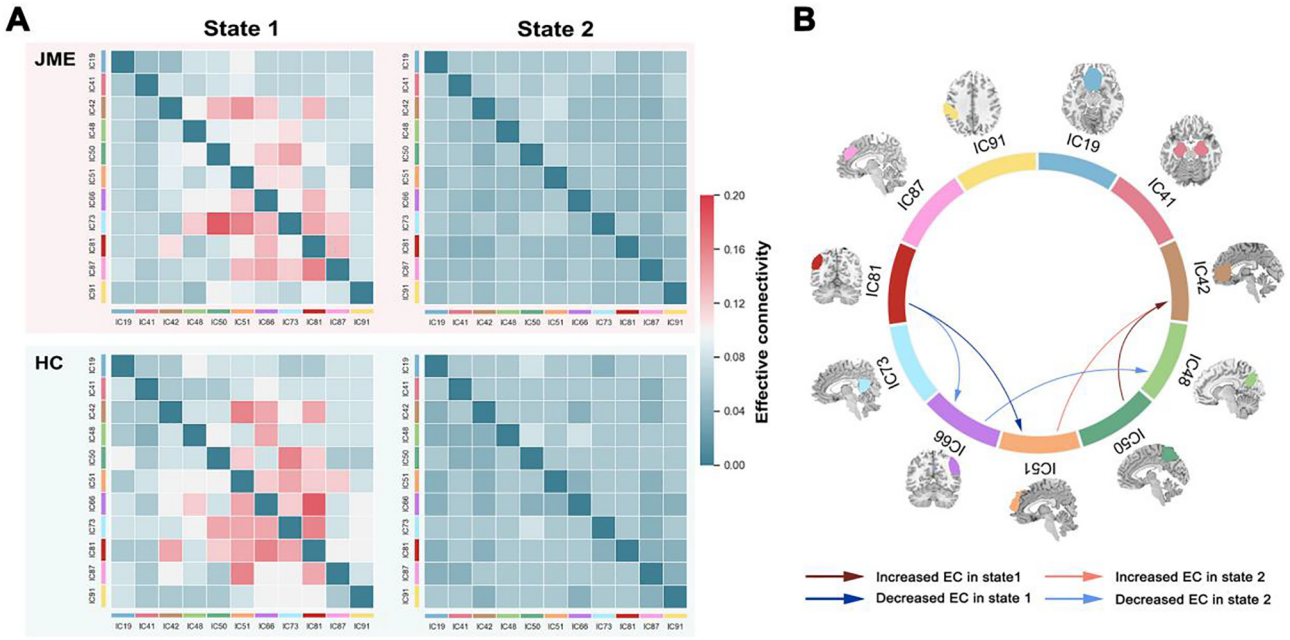

Fig. 4. Dynamic effective connectivity patterns for two groups. (A) Group-specific centroid matrices for each state. (B) State-specific group differences in centroid matrices ($P < 0.05$, FDR corrected). The arrows indicate the directions of causal influences. The lines with warm and cool colors indicate the increased and decreased effective connectivity (EC) in JME patients compared with HCs respectively. JME, juvenile myoclonic epilepsy; HC, healthy control; IC, independent component.

DM components, but significantly decreased out-weighted degree from IC81 to other DM components and in-out-weighted degree of IC51 ($P < 0.05$, FDR corrected). We further explored the temporal properties (fractional windows, number of transitions, and dwell time) in each group, but no significant between-group differences were found. The statistical results of these temporal properties are provided in

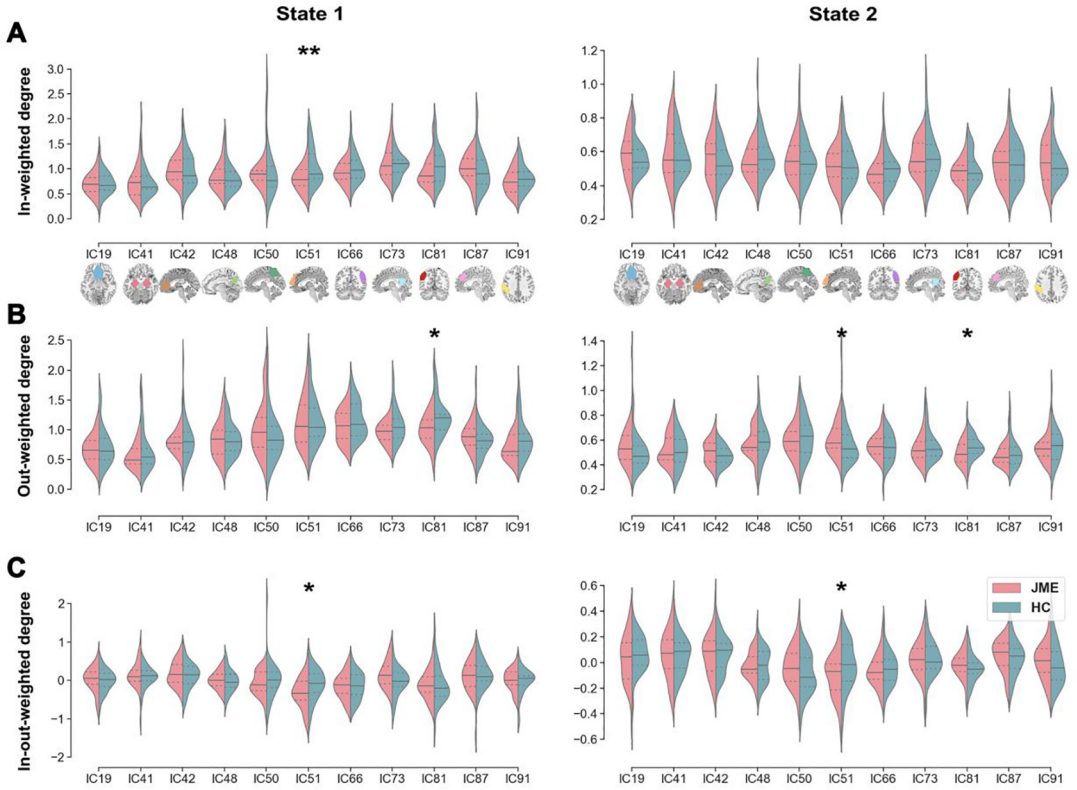

Fig. 5. Causal influence flows of dynamic effective connectivity. The in-weighted degree (A), out-weighted degree (B), and in-out weighted degree (C) in two states are shown using violin plots for JME patients (red) and HCs (green). Horizontal solid and dashed lines indicate group means and interquartile range respectively. ** and * represent $P < 0.01$ and $P < 0.05$ with FDR corrected. JME, juvenile myoclonic epilepsy; HC, healthy control; IC, independent component. (For interpretation of the references to color in this figure legend, the reader is referred to the web version of this article.)

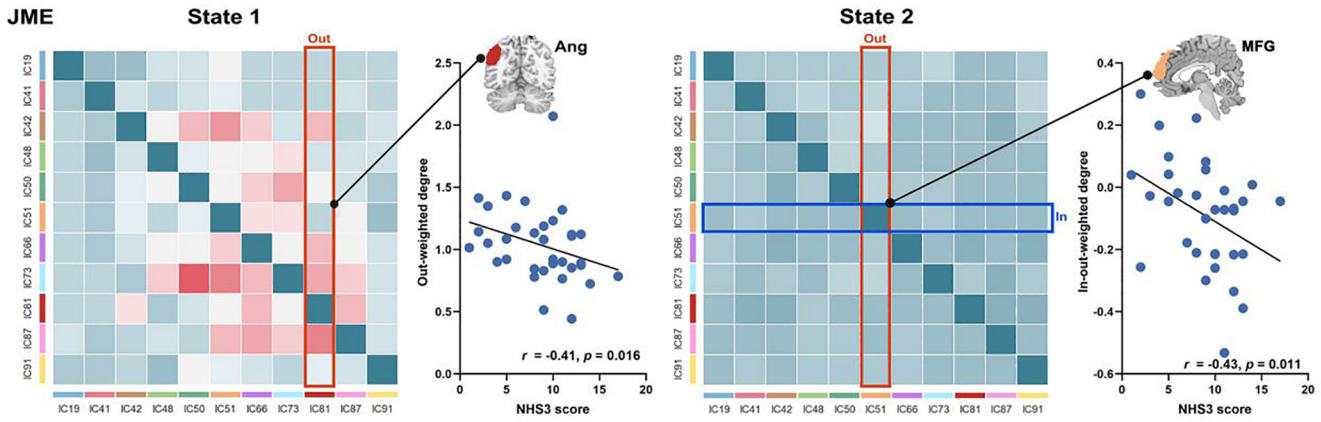

Fig. 6. Relationships between clinical features and causal influence flows. The red and blue rectangular boxes in the centroid matrix indicate the in and out causal influence flow of DM components. Ang, angular gyrus; MFG, medial frontal gyrus; JME, juvenile myoclonic epilepsy. (For interpretation of the references to color in this figure legend, the reader is referred to the web version of this article.)

Supplementary Figure S2.

3.4. Relationship with clinical disease severity

We first tested whether abnormal DEC patterns in patients with JME were associated with their clinical features, but did not find any significant correlations. We further explored the associations between abnormal causal influence flows and clinical features. As shown in Fig. 6, we found that the NHS3 total scores of patients were significantly correlated with out-weighted degree from IC81 to other DM components in State 1 (r = -0.41, P = 0.016, FDR corrected) and in-out-weighted degree of IC51 in State 2 (r = -0.43, P = 0.011, FDR corrected).

4. Discussion

In this study, we investigated the abnormalities of the dynamic causal influences within the DMN in newly diagnosed, drug-naïve JME. The primary findings are as follows: first, we found that the transient patterns of causal influences within the DMN have two distinct configurations, a less frequent, strongly-connected state (State 1) and a more frequent, weakly-connected state (State 2), across the two groups; second, compared with controls, patients with JME showed state-specific EC changes among several DMN regions, particularly exhibited altered ECs between DMN subnetworks in State 1 as well as abnormal ECs within DMN subnetworks in State 2; third, causal influence flows among DMN regions were also altered across two states and associated with the disease severity of JME assessed by the NHS3 score. All these results provide a new account of neuropsychological mechanisms of JME at the early phase of the disease.

The present work from the perspective of EC identified two distinct dynamic state profiles, a less frequent state characterized by strongly-connected inter-influence among DM components (State 1) and a more frequent state characterized by weakly-connected inter-influence among DM components (State 2). The identified states were in line with the dynamic FC patterns presented in prior findings (Chen et al., 2017). Indeed, dynamic FC analysis usually estimates and characterizes windowed FC matrices into several distinct connectivity states that represent the transient patterns of FC over time (Allen et al., 2014; Thompson, 2017). Although the underlying cognitive processes remains largely unknown, these diverse FC states are believed to reflect distinct internal states of the brain (e.g. a state of alertness or drowsiness), in terms of functional interactions (Calhoun and Adali, 2016; Lim et al., 2018; Zhou et al., 2019). This can be supported by the evidence that dynamic FC states derived from rs-fMRI are linked to discrete mental states observed in EEG measurements (Allen et al., 2018). Our results may extend to previous findings, suggesting that different causal influence patterns might also be related to discrete brain cognitive states during resting-state. Furthermore, previous research suggested that the DMN is in charge of both the internal thoughts and response to external stimuli in resting-state, and these two aspects can be reflected by distinct connective patterns of the DMN (Zuo et al., 2016) and related to the switches between different phases of attention (Scheibner et al., 2017). Considering the role of the DMN in supporting the internal mentation and monitoring the external environment, we can speculate that the State 1 may be an internal-oriented state which supports internally constructed representations, and the State 2 may be an external-oriented state which supports externally constrained representations. Our speculation can be supported by the findings of whole-brain dynamic network connectivity analyses that diverse dynamic FC states may reflect the forms of functional communication in the brain networks and thus support different cognitive processes (Fiorenzato et al., 2019; Kim et al., 2017). Future studies are needed to disentangle the relationships between these different states of the DMN and specific cognitive processing.

Patients in this study exhibited changed ECs among multiple DM components, specifically between the PCU (IC48 and IC50), ACC (IC42), MFG (IC51), and Ang (IC66 and IC81). The PCU is a key region of the DMN and associated with emotion regulation (Fransson and Marrelec, 2008). Previous studies have suggested that the PCU plays an important role in onset of spike-and-wave discharge in JME (Lee et al., 2014). Our altered ECs between PCU and other regions are in line with previous studies, which have revealed PCU-related dysconnectivity in JME (Jiang et al., 2018; Routley et al., 2020), suggesting a critical role of emotional dysregulation in the development of JME. The ACC is typically related to emotional processing (Etkin et al., 2011), and its alterations in structure and function have been revealed in patients with JME (Cao et al., 2013; Jiang et al., 2016). Our altered ECs of ACC suggest that atypical emotional processing has been implicated in the neuropsychology of JME. The MFG has been associated with internal mentation and self-reference processing (Northoff et al., 2006; Whitfield-Gabrieli et al., 2011). Previous studies have frequently reported dysconnectivity of MFG with motor system in patients with JME (Christian Vollmar et al., 2011, 2012). Consistently, our altered ECs of MFG suggest that abnormal internal cognitive process may contribute to myoclonic jerks in JME. In addition, the Ang is involved in social cognition and language (Bzdok et al., 2016; Seghier, 2013), and its dysconnectivity with other DMN regions has been reported in JME (McGill et al., 2012). Overall, the altered ECs among these DMN components may implicate neuropsychological impairments in patients with JME. More importantly, we found that these changed ECs were located between anterior (e.g. ACC and MFG) and posterior DMN (e.g.

PCU and Ang) regions in State 1, whereas within anterior and posterior DMN regions in State 2, suggesting state-specific abnormalities in EC patterns. Previous static FC studies have indicated that JME patients had lower mean connective strength between anterior and posterior DMN regions (Dong et al., 2016). The present study extends current research to temporal dynamic domain and further suggests that disrupted functional integration between DMN subnetworks may be dominated by an internal-oriented state, whereas disrupted functional segregation within DMN subnetworks may be dominated by an external-oriented state in patients.

Our results also showed that the causal influence flows related to MFG (IC51) and left Ang (IC81) have been altered across two states in the patient cohort, suggesting a disrupted role of these regions as a hub receptor and generator in functional interaction. Previous studies have demonstrated that the causal influence flows among the DMN regions were correlated with their neuronal activity levels (Jiao et al., 2011). The abnormal activity in the MFG and Ang have been widely found in JME (Bartolini et al., 2014; McGill et al., 2014), the altered causal influence flows of these regions may reflect disabilities in receiving and generating influences with other DMN regions. Interestingly, the MFG showed decreased in-weighted degree in Stated 1, whereas exhibited increased out-weighted degree in State 2, indicating state-specific alterations of causal influence flows in patients with JME. The MFG has been implicated in integrating the external environment with stored internal representations (Buckner et al., 2008), and the abnormal MFG connectivity is associated with abnormal internal representations on specific cognitive processes, such as attention, memory, and consciousness, for both chronic illness and newly diagnosed JME patients (Lee and Park, 2019; Maneshi et al., 2012). Also, the MFG is involved with the thalamo-cortical circuit, and its connectivity reduces with the basal ganglia reflects the disruption of external interaction which is related to executing voluntary movements in JME (O'Muircheartaigh et al., 2012). Our state-specific results suggest that, for patients with newly diagnosed drug-naïve JME, the MFG became less important in supporting internally constructed representations when it served as a hub receptor in the DMN; on the contrary, as a hub generator of the DMN, the MFG played a more important role in supporting externally constrained representations. This can be seen as a compensatory process, where the functional interaction decreases in an internal-oriented state while increases in an external-oriented state in patients with JME.

We also found that the altered causal influence flows were significantly correlated with NHS3 scores in patients with JME, suggesting the lower directed interactions are corresponding to the greater disease severity. These results were consistent with previous observations of associations between atypical brain dynamics and epileptic symptoms (Li et al., 2019; H. Liu et al., 2019). A recent study reported that patients with GTCS showed enhanced temporal variability of FC in large-scale brain functional networks, with these excessive variability anti-correlated with the duration of disease (Jia et al., 2020). Our previous study also suggested that reduced dynamics within and between RSNs were linked to greater disease severity in JME (Zhang et al., 2018). Taken together, the established associations in this study indicate that the early identified abnormalities in brain networks may be implicated in the progress of the disease, and can be an indication of disrupted developmental processes in JME.

Our study was subject to various considerations and limitations. First, although the GCA is considered to be an effective method for evaluating EC in rs-fMRI data, it has been claimed that the changes in directionality can be caused by the differences in hemodynamic coupling among different brain regions (Pervaiz et al., 2020). Recently, other models, particularly the dynamic causal model (DCM) - a hemodynamic model (Friston et al., 2014), have been proposed to detect dynamic EC among hidden neuronal states (Park et al., 2018b; Zarghami and Friston, 2020). Therefore, it would be interesting to see future attempts utilizing DCM to examine the reorganizations of dynamic EC in patients with ME. Second, previous studies have suggested that the epileptic transients may have significant effect on the functional connectivity (Bettus et al., 2011). However, in the present study, the EEG data was not recorded during rs-fMRI scanning since it is difficult for participants to continue to not move their head during scanning. In the future, it would be important to evaluate the influence of the interictal epileptic discharges on dynamic brain networks by using a simultaneous EEG-fMRI analysis. Third, in order to investigate the intrinsic disease process on reorganization of dynamic EC rather than the effect of direct pharmacological treatment, we opted for a homogeneous cohort of newly diagnosed drug-naïve JME. Although this is an advantage of the study, our sample size is subsequently small. Our sample size was comparable with other recent studies that examined patients with newly diagnosed JME (Lee an Park, 2019) and dynamic FC (Wang et al., 2019). Nonetheless, further study with a larger sample set is needed to investigate the replicability of our findings.

5. Conclusion

The current study adopts a novel DEC method that combined a sliding window approach with a multivariate Granger causality analysis to study the dynamic alterations of causal influence within the DMN in patients with newly diagnosed and drug-naïve JME. Our results showed that temporal patterns of causal influences within the DMN are altered in patients, and were associated with clinical symptoms in patients. Our findings extend current research regarding the DMN disruption in JME patients and suggest that dynamic effective connectivity could be a potential way to uncover the pathophysiology of JME at the early phase of illness.

6. Contributor's statements

ZZ designed the study and performed statistical analyses, drafted the manuscript, and approved the final manuscript as submitted. GL performed the MRI data acquisition and the neuropsychological assessment, statistical analyses, and approved the final manuscript as submitted. WZ, JS, and HL coordinated and carried out the data collection, revised the manuscript, and approved the final manuscript as submitted. YS conceptualized the study, critically reviewed the manuscript, and approved the final manuscript as submitted.

7. Source of funding

This work was supported by the National Natural Science Foundation of China (No.81801785), by the "Hundred Talents Program" of Zhejiang University, by the Fundamental Research Funds for the Central Universities (No. 2019FZJD005 and 2020FZZX001-05), by the Zhejiang Lab (No. 2019KE0AD01), by the Gansu Province Universities and Colleges Scientific Research Project (No. 2018A-124), by the China Postdoctoral Science Foundation (No. 2202M671727), by the Postdoctoral Science Foundation of Zhejiang Province (No. 514000-X81901), by the Cuiying Scientific and Technological Innovation Program of Lanzhou University Second Hospital (No. CY2018-QN03), and by the Innovation Capacity Improvement Project of Colleges and Universities in Gansu Province (No. 2019B-015).

CRediT authorship contribution statement

Zhe Zhang: Conceptualization, Methodology, Investigation, Results interpretation, Formal analysis, Writing - original draft, Writing - review & editing. **Guangyao Liu:** Data collection, Neuropsychological assessment, Methodology, Results interpretation. **Weihao Zheng:** Writing - review & editing. **Jie Shi:** Writing - review & editing. **Hong Liu:** Data collection, Writing - review & editing. **Yu Sun:** Conceptualization, Supervision, Results interpretation, Writing - review & editing.

Acknowledgments

We would like to thank all subjects in this study.

Statement of datasharing

The data that support the findings of this study are available from the corresponding author upon reasonable request.

Disclosures

Neither of the authors has any conflict of interest to disclose.

Appendix A. Supplementary data

Supplementary data to this article can be found online at https://doi.org/10.1016/j.nicl.2020.102431.

References

Aggarwal, C.C., Hinneburg, A., Keim, D.A., 2001. On the Surprising Behavior of Distance Metrics in High Dimensional Space. Springer, New York, NY.

Akansha, M., Roberto, A.J., Abhishek, M., Aileen, L., Kathryn, J., Carney, M.J., 2016. The significance of the default mode network (DMN) in neurological and neuropsychiatric disorders: a review. Yale J. Biol. Med. 89 (1), 49–57.

Allen, E.A., Damaraju, E., Eichele, T., Wu, L., Calhoun, V.D., 2018. EEG signatures of dynamic functional network connectivity states. Brain Topogr. 31 (1), 101–116. https://doi.org/10.1007/s10548-017-0546-2.

Allen, E.A., Damaraju, E., Plis, S.M., Erhardt, E.B., Eichele, T., Calhoun, V.D., 2014. Tracking whole-brain connectivity dynamics in the resting state. Cereb. Cortex 24 (3), 663–676. https://doi.org/10.1093/cercor/bhs352.

Allen, E.A., Erhardt, E.B., Damaraju, E., Gruner, W., Segall, J.M., Silva, R.F., et al., 2011. A baseline for the multivariate comparison of resting-state networks. Front. Syst. Neurosci. 5, 2. https://doi.org/10.3389/fnsys.2011.00002.

Bartolini, E., Pesaresi, I., Fabbri, S., Cecchi, P., Giorgi, F.S., Sartucci, F., et al., 2014. Abnormal response to photic stimulation in Juvenile Myoclonic Epilepsy: An EEG-fMRI study. Epilepsia 55 (7), 1038–1047. https://doi.org/10.1111/epi.12634.

Baykan, B., Wolf, P., 2017. Juvenile myoclonic epilepsy as a spectrum disorder: A focused review. Seizure 49, 36–41. https://doi.org/10.1016/j.seizure.2017.05.011.

Bell, A.J., Sejnowski, T.J., 1995. An information-maximization approach to blind separation and blind deconvolution. Neural Computing 7 (6), 1129–1159.

Bettus, G., Ranjeva, J.P., Wendling, F., Bénar, C.G., Confortgouny, S., Régis, J., et al., 2011. Interictal functional connectivity of human epileptic networks assessed by intracerebral eeg and bold signal fluctuations. PLoS ONE 6 (5), e20071. https://doi.org/10.1371/journal.pone.0020071.g001.

Buckner, R.L., Andrews-Hanna, J.R., Schacter, D.L., 2008. The brain's default network: anatomy, function, and relevance to disease. Ann. N. Y. Acad. Sci. 1124, 1–38. https://doi.org/10.1196/annals.1440.011.

Buckner, R.L., DiNicola, L.M., 2019. The brain's default network: updated anatomy, physiology and evolving insights. Nat. Rev. Neurosci. 20 (10), 593–608. https://doi.org/10.1038/s41583-019-0212-7.

Bzdok, D., Hartwigsen, G., Reid, A., Laird, A.R., Fox, P.T., Eickhoff, S.B., 2016. Left inferior parietal lobe engagement in social cognition and language. Neurosci. Biobehav. Rev. 68, 319–334. https://doi.org/10.1016/j.neubiorev.2016.02.024.

Caciagli, L., Wandschneider, B., Xiao, F., Vollmar, C., Centeno, M., Vos, S.B., et al., 2019. Abnormal hippocampal structure and function in juvenile myoclonic epilepsy and unaffected siblings. Brain 142 (9), 2670–2687. https://doi.org/10.1093/brain/awz215.

Calhoun, V.D., Adali, T., 2016. Time-varying brain connectivity in fmri data: whole-brain data-driven approaches for capturing and characterizing dynamic states. IEEE Signal Process Mag. 33 (3), 52–66. https://doi.org/10.1109/MSP.2015.2478915.

Calhoun, V.D., Miller, R., Pearlson, G., Adali, T., 2014. The chronnectome: time-varying connectivity networks as the next frontier in fMRI data discovery. Neuron 84 (2), 262–274. https://doi.org/10.1016/j.neuron.2014.10.015.

Cao, B., Tang, Y., Li, J., Zhang, X., Shang, H.F., Zhou, D., 2013. A meta-analysis of voxel-based morphometry studies on gray matter volume alteration in juvenile myoclonic epilepsy. Epilepsy Res. 106 (3), 370–377. https://doi.org/10.1016/j.eplepsyres.2013.07.003.

Carvalho, K.C., Uchida, C.G., Guaranha, M.S., Guilhoto, L.M., Wolf, P., Yacubian, E.M., 2016. Cognitive performance in juvenile myoclonic epilepsy patients with specific endophenotypes. Seizure 40, 33–41. https://doi.org/10.1016/j.seizure.2016.06.002.

Chen, H.J., Lin, H.L., Chen, Q.F., Liu, P.F., 2017. Altered dynamic functional connectivity in the default mode network in patients with cirrhosis and minimal hepatic encephalopathy. Neuroradiology 59 (9), 905–914. https://doi.org/10.1007/s00234-017-1881-4.

Damaraju, E., Allen, E.A., Belger, A., Ford, J.M., McEwen, S., Mathalon, D.H., et al., 2014. Dynamic functional connectivity analysis reveals transient states of dysconnectivity in schizophrenia. Neuroimage Clin 5, 298–308. https://doi.org/10.1016/j.nicl.2014.07.003.

David, O., Guillemain, I., Saillet, S., Reyt, S., Deransart, C., Segebarth, C., Depaulis, A., 2008. Identifying neural drivers with functional MRI: an electrophysiological validation. PLoS Biol. 6 (12), 2683–2697. https://doi.org/10.1371/journal.pbio.0060315.

Deshpande, G., Hu, X., 2012. Investigating Effective Brain Connectivity from fMRI Data: Past Findings and Current Issues with Reference to Granger Causality Analysis. Brain Connect. 2 (5), 235–245. https://doi.org/10.1089/brain.2012.0091.

Dobryakova, E., Rocca, M.A., Valsasina, P., DeLuca, J., Filippi, M., 2017. Altered neural mechanisms of cognitive control in patients with primary progressive multiple sclerosis: An effective connectivity study. Hum. Brain Mapp. 38 (5), 2580–2588. https://doi.org/10.1002/hbm.23542.

Dong, L., Luo, C., Zhu, Y., Hou, C., Jiang, S., Wang, P., et al., 2016. Complex discharge-affecting networks in juvenile myoclonic epilepsy: A simultaneous EEG-fMRI study. Hum. Brain Mapp. 37 (10), 3515–3529. https://doi.org/10.1002/hbm.23256.

Etkin, A., Egner, T., Kalisch, R., 2011. Emotional processing in anterior cingulate and medial prefrontal cortex. Trends Cogn Sci 15 (2), 85–93. https://doi.org/10.1016/j.tics.2010.11.004.

Fiorenzato, E., Strafella, A.P., Kim, J., Schifano, R., Weis, L., Antonini, A., Biundo, R., 2019. Dynamic functional connectivity changes associated with dementia in Parkinson's disease. Brain 142 (9), 2860–2872. https://doi.org/10.1093/brain/awz192.

Fransson, P., Marrelec, G., 2008. The precuneus/posterior cingulate cortex plays a pivotal role in the default mode network: Evidence from a partial correlation network analysis. Neuroimage 42 (3), 1178–1184. https://doi.org/10.1016/j.neuroimage.2008.05.059.

Friston, K.J., 2011. Functional and effective connectivity: a review. Brain Connect. 1 (1), 13–36. https://doi.org/10.1089/brain.2011.0008.

Friston, K.J., Kahan, J., Biswal, B., Razi, A., 2014. A DCM for resting state fMRI. Neuroimage 94, 396–407. https://doi.org/10.1016/j.neuroimage.2013.12.009.

Fu, Z., Tu, Y., Di, X., Du, Y., Sui, J., Biswal, B.B., et al., 2019. Transient increased thalamic-sensory connectivity and decreased whole-brain dynamism in autism. Neuroimage 190, 191–204. https://doi.org/10.1016/j.neuroimage.2018.06.003.

Gleichgerrcht, E., Kocher, M., Bonilha, L., 2015. Connectomics and graph theory analyses: Novel insights into network abnormalities in epilepsy. Epilepsia 56 (11), 1660–1668. https://doi.org/10.1111/epi.13133.

Hamilton, J.P., Chen, G., Thomason, M.E., Schwartz, M.E., Gotlib, I.H., 2011. Investigating neural primacy in Major Depressive Disorder: multivariate Granger causality analysis of resting-state fMRI time-series data. Mol. Psychiatry 16 (7), 763–772. https://doi.org/10.1038/mp.2010.46.

Inanaga, K., Ohtahara, S., Seino, M., 1985. On the Proposal for Classification of Epilepsies and Epileptic Syndromes. Psychiatry Clin. Neurosci. 39 (3), 333–335. https://doi.org/10.1111/j.1440-1819.1985.tb02013.x.

Jia, X., Ma, S., Jiang, S., Sun, H., Dong, D., Chang, X., et al., 2018. Disrupted Coupling Between the Spontaneous Fluctuation and Functional Connectivity in Idiopathic Generalized Epilepsy. Front. Neurol. 9. https://doi.org/10.3389/fneur.2018.00838.

Jia, X., Xie, Y., Dong, D., Pei, H., Jiang, S., Ma, S., et al., 2020. Reconfiguration of dynamic large-scale brain network functional connectivity in generalized tonic-clonic seizures. Hum. Brain Mapp. 41 (1), 67–79. https://doi.org/10.1002/hbm.24787.

Jiang, S., Luo, C., Gong, J., Peng, R., Ma, S., Tan, S., et al., 2018. Aberrant Thalamocortical Connectivity in Juvenile Myoclonic Epilepsy. Int. J. Neural Syst. 28 (1). https://doi.org/10.1142/s0129065717500344.

Jiang, S., Luo, C., Liu, Z., Hou, C., Wang, P., Dong, L., et al., 2016. Altered Local Spontaneous Brain Activity in Juvenile Myoclonic Epilepsy: A Preliminary Resting-State fMRI Study. Neural Plast 2016, 3547203. https://doi.org/10.1155/2016/3547203.

Jiao, Q., Lu, G., Zhang, Z., Zhong, Y., Wang, Z., Guo, Y., et al., 2011. Granger causal influence predicts BOLD activity levels in the default mode network. Hum. Brain Mapp. 32 (1), 154–161. https://doi.org/10.1002/hbm.21065.

Jr, E.J., 2001. A proposed diagnostic scheme for people with epileptic seizures and with epilepsy: report of the ilae task force on classification and terminology. Epilepsia 42 (6), 796–803. https://doi.org/10.1046/j.1528-1157.2001.10401.x.

Kim, J., Criaud, M., Cho, S.S., Mihaescu, A., Coakeley, S., Ghadery, C., et al., 2017. Abnormal intrinsic brain functional network dynamics in Parkinson's disease. Brain 140, 2955–2967. https://doi.org/10.1093/brain/awx233/4320219.

Koepp, M.J., Thomas, R.H., Wandschneider, B., Berkovic, S.F., Schmidt, D., 2014. Concepts and controversies of juvenile myoclonic epilepsy: still an enigmatic epilepsy. Expert Rev. Neurother. 14 (7), 819–831. https://doi.org/10.1586/14737175.2014.928203.

Lee, C., Kim, S.M., Jung, Y.J., Im, C.H., Kim, D.W., Jung, K.Y., 2014. Causal influence of epileptic network during spike-and-wave discharge in juvenile myoclonic epilepsy. Epilepsy Res. 108 (2), 257–266. https://doi.org/10.1016/j.eplepsyres.2013.11.005.

Lee, H.J., Park, K.M., 2019. Structural and functional connectivity in newly diagnosed juvenile myoclonic epilepsy. Acta Neurol. Scand. 139 (5), 469–475. https://doi.org/10.1111/ane.13079.

Li, R., Wang, L., Chen, H., Guo, X., Liao, W., Tang, Y.L., Chen, H., 2019. Abnormal dynamics of functional connectivity density in children with benign epilepsy with centrotemporal spikes. Brain Imaging Behav 13 (4), 985–994. https://doi.org/10.1007/s11682-018-9914-0.

Liao, W., Ding, J., Marinazzo, D., Xu, Q., Wang, Z., Yuan, C., et al., 2011. Small-world directed networks in the human brain: multivariate Granger causality analysis of resting-state fMRI. Neuroimage 54 (4), 2683–2694. https://doi.org/10.1016/j.neuroimage.2010.11.007.

Liao, W., Zhang, Z., Mantini, D., Xu, Q., Ji, G.J., Zhang, H., et al., 2014. Dynamical intrinsic functional architecture of the brain during absence seizures. Brain Struct. Funct. 219 (6), 2001–2015. https://doi.org/10.1007/s00429-013-0619-2.

Lim, J., Teng, J., Patanaik, A., Tandi, J., Massar, S.A.A., 2018. Dynamic functional connectivity markers of objective trait mindfulness. Neuroimage 176, 193–202. https://

doi.org/10.1016/j.neuroimage.2018.04.056.
Liu, F., Wang, Y., Li, M., Wang, W., Li, R., Zhang, Z., et al., 2017. Dynamic functional network connectivity in idiopathic generalized epilepsy with generalized tonic-clonic seizure. Hum. Brain Mapp. 38 (2), 957–973. https://doi.org/10.1002/hbm.23430.
Liu, H., Li, W., Zhao, M., Wu, J., Wu, J., Yang, J., Jiao, B., 2019. Altered temporal dynamics of brain activity in patients with generalized tonic-clonic seizures. PLoS ONE 14 (7), e0219904. https://doi.org/10.1371/journal.pone.0219904.
Lurie, D.J., Kessler, D., Bassett, D.S., Betzel, R.F., Breakspear, M., Kheilholz, S., et al., 2020. Questions and controversies in the study of time-varying functional connectivity in resting fMRI. Network Neurosci. 4 (1), 30–69. https://doi.org/10.1162/netn_a_00116.
Malhi, G.S., Das, P., Outhred, T., Bryant, R.A., Calhoun, V., 2019. Resting-state neural network disturbances that underpin the emergence of emotional symptoms in adolescent girls: resting-state fMRI study. Br. J. Psychiatry 215 (3), 545–551. https://doi.org/10.1192/bjp.2019.10.
Maneshi, M., Moeller, F., Fahoum, F., Gotman, J., Grova, C., 2012. Resting-State Connectivity of the Sustained Attention Network Correlates with Disease Duration in Idiopathic Generalized Epilepsy. PLoS ONE 7 (12). https://doi.org/10.1371/journal.pone.0050359.
Mason, M.F., Norton, M.I., Van Horn, J.D., Wegner, D.M., Grafton, S.T., Macrae, C.N., 2007. Wandering minds: the default network and stimulus-independent thought. Science 315 (5810), 393–395. https://doi.org/10.1126/science.1131295.
Mastrovito, D., Hanson, C., Hanson, S.J., 2018. Differences in atypical resting-state effective connectivity distinguish autism from schizophrenia. Neuroimage Clin 18, 367–376. https://doi.org/10.1016/j.nicl.2018.01.014.
McGill, M.L., Devinsky, O., Kelly, C., Milham, M., Castellanos, F.X., Quinn, B.T., et al., 2012. Default mode network abnormalities in idiopathic generalized epilepsy. Epilepsy Behav. 23 (3), 353–359. https://doi.org/10.1016/j.yebeh.2012.01.013.
McGill, M.L., Devinsky, O., Wang, X., Quinn, B.T., Pardoe, H., Carlson, C., et al., 2014. Functional neuroimaging abnormalities in idiopathic generalized epilepsy. Neuroimage-Clinical 6, 455–462. https://doi.org/10.1016/j.nicl.2014.10.008.
Northoff, G., Heinzel, A., de Greck, M., Bermpohl, F., Dobrowolny, H., Panksepp, J., 2006. Self-referential processing in our brain–a meta-analysis of imaging studies on the self. Neuroimage 31 (1), 440–457. https://doi.org/10.1016/j.neuroimage.2005.12.002.
O 'Donoghue, M.F., Duncan, J.S., Sander, J.W.A.S., 1996. The National Hospital Seizure Severity Scale: A Further Development of the Chalfont Seizure Severity Scale. Epilepsia 37 (6), 563–571.
O'Muircheartaigh, J., Vollmar, C., Barker, G.J., Kumari, V., Symms, M.R., Thompson, P., et al., 2012. Abnormal thalamocortical structural and functional connectivity in juvenile myoclonic epilepsy. Brain 135, 3635–3644. https://doi.org/10.1093/brain/aws296.
Panayiotopoulos, C.P., Obeid, T., Tahan, A.R., 1994. Juvenile myoclonic epilepsy: a 5-year prospective study. Epilepsia 35, 285–296.
Park, C.H., Choi, Y.S., Kim, H.J., Chung, H.K., Jung, A.R., Yoo, J.H., Lee, H.W., 2018a. Interactive effects of seizure frequency and lateralization on intratemporal effective connectivity in temporal lobe epilepsy. Epilepsia 59 (1), 215–225. https://doi.org/10.1111/epi.13951.
Park, H.J., Friston, K.J., Pae, C., Park, B., Razi, A., 2018b. Dynamic effective connectivity in resting state fMRI. Neuroimage 180 (SI), 594–608. https://doi.org/10.1016/j.neuroimage.2017.11.033.
Parsons, N., Bowden, S.C., Vogrin, S., D'Souza, W.J., 2020. Default mode network dysfunction in idiopathic generalised epilepsy. Epilepsy Res. 159. https://doi.org/10.1016/j.eplepsyres.2019.106254.
Pascalicchio, T.F., de Araujo Filho, G.M., da Silva Noffs, M.H., Lin, K., Caboclo, L.O., Vidal-Dourado, M., et al., 2007. Neuropsychological profile of patients with juvenile myoclonic epilepsy: a controlled study of 50 patients. Epilepsy Behav. 10 (2), 263–267. https://doi.org/10.1016/j.yebeh.2006.11.012.
Paulus, F.M., Krach, S., Blanke, M., Roth, C., Belke, M., Sommer, J., et al., 2015. Fronto-insula network activity explains emotional dysfunctions in juvenile myoclonic epilepsy: combined evidence from pupillometry and fMRI. Cortex 65, 219–231. https://doi.org/10.1016/j.cortex.2015.01.018.
Pervaiz, U., Vidaurre, D., Woolrich, M.W., Smith, S.M., 2020. Optimising network modelling methods for fMRI. Neuroimage 211, 116604. https://doi.org/10.1016/j.neuroimage.2020.116604.
Routley, B., Shaw, A., Muthukumaraswamy, S.D., Singh, K.D., Hamandi, K., 2020. Juvenile myoclonic epilepsy shows increased posterior theta, and reduced sensorimotor beta resting connectivity. Epilepsy Res. 163, 106324. https://doi.org/10.1016/j.eplepsyres.2020.106324.
Scheffer, I.E., Berkovic, S., Capovilla, G., Connolly, M.B., French, J., Guilhoto, L., et al., 2017. ILAE classification of the epilepsies: Position paper of the ILAE Commission for Classification and Terminology. Epilepsia 58 (4), 512–521. https://doi.org/10.1111/epi.13709.
Scheibner, H.J., Bogler, C., Gleich, T., Haynes, J.D., Bermpohl, F., 2017. Internal and external attention and the default mode network. Neuroimage 148, 381–389. https://doi.org/10.1016/j.neuroimage.2017.01.044.
Seghier, M.L., 2013. The angular gyrus: multiple functions and multiple subdivisions. Neuroscientist 19 (1), 43–61. https://doi.org/10.1177/1073858412440596.
Sladky, R., Hoflich, A., Kublbock, M., Kraus, C., Baldinger, P., Moser, E., et al., 2015. Disrupted effective connectivity between the amygdala and orbitofrontal cortex in social anxiety disorder during emotion discrimination revealed by dynamic causal modeling for FMRI. Cereb. Cortex 25 (4), 895–903. https://doi.org/10.1093/cercor/bht279.
Stevens, M.C., Pearlson, G.D., Calhoun, V.D., 2009. Changes in the interaction of resting-state neural networks from adolescence to adulthood. Hum. Brain Mapp. 30 (8), 2356–2366. https://doi.org/10.1002/hbm.20673.
Thompson, G.J., 2017. Neural and metabolic basis of dynamic resting state fMRI. Neuroimage 180 (SI), 448–462. https://doi.org/10.1016/j.neuroimage.2017.09.010.
Tu, Y., Fu, Z., Zeng, F., Maleki, N., Lan, L., Li, Z., et al., 2019. Abnormal thalamocortical network dynamics in migraine. Neurology 92 (23), e2706–e2716. https://doi.org/10.1212/WNL.0000000000007607.
Vollmar, C., O'Muircheartaigh, J., Barker, G.J., Symms, M.R., Thompson, P., Kumari, V., et al., 2011. Motor system hyperconnectivity in juvenile myoclonic epilepsy: a cognitive functional magnetic resonance imaging study. Brain 134, 1710–1719. https://doi.org/10.1093/brain/awr098.
Vollmar, C., O'Muircheartaigh, J., Symms, M.R., Barker, G.J., Thompson, P., Kumari, V., et al., 2012. Altered microstructural connectivity in juvenile myoclonic epilepsy The missing link. Neurology 78 (20), 1555–1559. https://doi.org/10.1212/WNL.0b013e3182563b44.
Wandschneider, B., Hong, S.J., Bernhardt, B.C., Fadaie, F., Vollmar, C., Koepp, M.J., et al., 2019. Developmental MRI markers cosegregate juvenile patients with myoclonic epilepsy and their healthy siblings. Neurology 93 (13), e1272–e1280. https://doi.org/10.1212/WNL.0000000000008173.
Wandschneider, B., Thompson, P.J., Vollmar, C., Koepp, M.J., 2012. Frontal lobe function and structure in juvenile myoclonic epilepsy: a comprehensive review of neuropsychological and imaging data. Epilepsia 53 (12), 2091–2098. https://doi.org/10.1111/epi.12003.
Wang, Y., Berglund, I.S., Uppman, M., Li, T.-Q., 2019. Juvenile myoclonic epilepsy has hyper dynamic functional connectivity in the dorsolateral frontal cortex. Neuroimage-Clinical 21. https://doi.org/10.1016/j.nicl.2018.11.014.
Whitfield-Gabrieli, S., Moran, J.M., Nieto-Castanon, A., Triantafyllou, C., Saxe, R., Gabrieli, J.D., 2011. Associations and dissociations between default and self-reference networks in the human brain. Neuroimage 55 (1), 225–232. https://doi.org/10.1016/j.neuroimage.2010.11.048.
Wolf, P., Yacubian, E.M., Avanzini, G., Sander, T., Schmitz, B., Wandschneider, B., Koepp, M., 2015. Juvenile myoclonic epilepsy: A system disorder of the brain. Epilepsy Res. 114, 2–12. https://doi.org/10.1016/j.eplepsyres.2015.04.008.
Yao, Z., Shi, J., Zhang, Z., Zheng, W., Hu, T., Li, Y., et al., 2019. Altered dynamic functional connectivity in weakly-connected state in major depressive disorder. Clin. Neurophysiol. 130 (11), 2096–2104. https://doi.org/10.1016/j.clinph.2019.08.009.
Zarghami, T.S., Friston, K.J., 2020. Dynamic effective connectivity. Neuroimage 207, 116453. https://doi.org/10.1016/j.neuroimage.2019.116453.
Zhang, Z., Liu, G., Yao, Z., Zheng, W., Xie, Y., Hu, T., et al., 2018. Changes in Dynamics Within and Between Resting-State Subnetworks in Juvenile Myoclonic Epilepsy Occur at Multiple Frequency Bands. Front. Neurol. 9, 448. https://doi.org/10.3389/fneur.2018.00448.
Zhong, C., Liu, R., Luo, C., Jiang, S., Dong, L., Peng, R., et al., 2018. Altered Structural and Functional Connectivity of Juvenile Myoclonic Epilepsy: An fMRI Study. Neural Plast. https://doi.org/10.1155/2018/7392187.
Zhou, Q., Zhang, L., Feng, J., Lo, C.Z., 2019. Tracking the Main States of Dynamic Functional Connectivity in Resting State. Front. Neurosci. 13, 685. https://doi.org/10.3389/fnins.2019.00685.
Zuo, N., Song, M., Fan, L., Eickhoff, S.B., Jiang, T., 2016. Different interaction modes for the default mode network revealed by resting state functional magnetic resonance imaging. Eur. J. Neurosci. 43 (1), 78–88. https://doi.org/10.1111/ejn.13112.